Morphology, Surface Structure, and Elastic Properties of PBT-Based Copolyesters with PEO-*b*-PEB-*b*-PEO Triblock Copolymer Soft Segments

Holger Schmalz,[†] Viola van Guldener,[‡] Wouter Gabriëlse,[‡] Ronald Lange,*[,‡,§] and Volker Abetz*[,†]

Makromolekulare Chemie II, Universität Bayreuth, 95440 Bayreuth, Germany, and DSM Research, P.O. Box 18, 6160 MD Geleen, The Netherlands

Received November 15, 2001

ABSTRACT: The elasticity of commonly known poly(butylene terephthalate)−poly(tetramethylene oxide) (PBT−PTMO)-based copoly(ether ester)s is increased by replacement of PTMO soft segments with poly(ethylene oxide)-*block*-poly(ethylene-*stat*-butylene)-*block*-poly(ethylene oxide) (PEO-*b*-PEB-*b*-PEO) triblock copolymer soft segments containing a nonpolar middle block based on hydrogenated polybutadiene (PEB). The incorporation of this strongly incompatible PEB block resulted in the aimed increased phase separation between the PBT hard blocks and the soft segment phase, leading to a disperse PBT phase and hence to an increased elasticity. Dynamic shear experiments in combination with small-angle X-ray scattering revealed that crystallization of the PBT hard segments occurs from a microphase-separated melt. The resulting dispersed PBT hard phase in these materials is shown using transmission electron microscopy (TEM) and scanning force microscopy (SFM), whereas the increased elasticity is demonstrated using mechanical characterization. Hysteresis measurements reveal that the plastic deformation after recovery from 100% strain is only 1−6% (depending on composition) for the new PEB-containing copolyesters compared to 33% for a PBT−PTMO-based copoly(ether ester). The combination of results obtained with differential scanning calorimetry (DSC) and dynamic mechanical analysis (DMA) points toward a complex morphology for the PEB-containing copolyesters. Five different phases exist: a crystalline pure PBT phase, pure amorphous PEB, and PBT phases and a PEO-rich phase besides an amorphous mixed PEO/PBT phase.

Introduction

Thermoplastic elastomers (TPE's) combine the properties of irreversibly cross-linked elastomers with the easy processing of thermoplastic materials. This enables product designs not easily achieved for conventional rubbers. One class of TPE's are copoly(ether ester)s or TPE-E's.[1] These segmented block copolymers possess a soft elastomeric polyether segment, e.g., poly(tetramethylene oxide) (PTMO) and a polyester hard segment, e.g., poly(butylene terephthalate) (PBT). Because of their phase-separated morphology, copoly(ether ester)s show unique properties such as good low-temperature flexibility and excellent mechanical properties up to high temperatures as well as a good resistance toward many solvents. However, the elastic properties of copoly(ether ester)s at relatively high elongations are limited. This is due to the presence of a co-continuous PBT hard phase as was revealed by morphological and mechanical characterization. The morphology of PBT−PTMO-based copoly(ether ester)s has been studied extensively.[1−7] It is generally assumed that, upon cooling from the homogeneous PBT−PTMO melt, the crystallization of PBT initiates the formation of the characteristic phase-separated structure consisting of PBT crystallites embedded in an amorphous matrix.[7,8] Although the crystallization process and the structure of the crystalline phase have been studied in detail (next to lamellar,[2,9−11] spherulitic,[5,6,12,13] dendritic,[6,13] even shish-kebab[6] structures have been reported), much less attention was paid to the structure of the amorphous phase. It is thought that this amorphous phase is homogeneous, resulting in the description of the copoly(ether ester)s by a two-phase model: a crystalline PBT phase and a homogeneous amorphous PTMO/noncrystalline PBT phase, both being co-continuous.[1−3,6] However, more recent studies using solid-state NMR[14] and thermomechanical analysis[15] demonstrate that the amorphous phase is not homogeneous but consists of a PTMO-rich phase and a PBT/PTMO mixed phase.

The relatively high modulus obtained in a stress−strain experiment reflects the presence of the co-continuous PBT morphology in copoly(ether ester)s. The stress−strain curves of copoly(ether ester)s can be divided into three distinct regions.[2] At low elongations a reversible elastic deformation of the co-continuous crystalline PBT matrix is obtained. At higher strains this co-continuous PBT matrix is disrupted along with orientation of the crystalline lamellae. This process is irreversible and results in the high plastic deformation hampering the elastic recovery, which is typical for these materials.[16] Finally, after crystallite orientation is completed the stress is submitted through the continuous amorphous phase, until it breaks. The general idea is that the elasticity of copoly(ether ester)s could be improved by changing the co-continuous PBT hard phase into a disperse phase. This can be achieved by increasing the phase separation as was demonstrated in thermoplastic polyurethanes or TPE-U's[17,18] and in strongly phase-separated copoly(ether ester aramides).[19] Incorporation of a nonpolar hydrogenated polybutadiene

[†] Universität Bayreuth.
[‡] DSM Research.
[§] Present address: BASF Aktiengesellschaft, GKS/B1, 67056 Ludwigshafen, Germany.
* Corresponding authors. E-mail: volker.abetz@uni-bayreuth.de; ronald.lange@basf-ag.de.

10.1021/ma011995o CCC: $22.00
Published on Web 06/06/2002

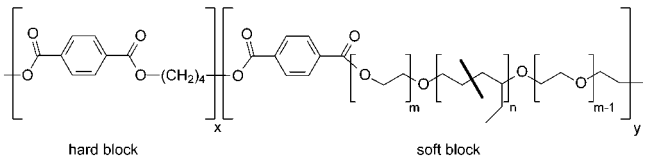

Figure 1. Structure of copolyesters with PEO-*b*-PEB-*b*-PEO soft segments.

Table 1. Composition of Copolyesters

	w(PBT) [%]	x_{HS}[a]	l_{HS}[b]	soft segment
PBT1000/50	50	0.837	6.1	PTMO
PBT45-1000	45	0.954	21.8	$PEO_{18}PEB_{64}PEO_{18}^{5.6}$
PBT40-1000	40	0.944	17.9	$PEO_{18}PEB_{64}PEO_{18}^{5.6}$
PBT35-1000	35	0.932	14.7	$PEO_{18}PEB_{64}PEO_{18}^{5.6}$
PBT30-1000	30	0.916	11.9	$PEO_{18}PEB_{64}PEO_{18}^{5.6}$
PBT25-1000	25	0.894	9.5	$PEO_{18}PEB_{64}PEO_{18}^{5.6}$
PBT20-1000	20	0.864	7.4	$PEO_{18}PEB_{64}PEO_{18}^{5.6}$
PBT40-1380	40	0.951	20.2	$PEO_{22}PEB_{56}PEO_{22}^{6.4}$
PBT30-1380	30	0.925	13.4	$PEO_{22}PEB_{56}PEO_{22}^{6.4}$
PBT20-1380	20	0.878	8.2	$PEO_{22}PEB_{56}PEO_{22}^{6.4}$

[a] Mole fraction of hard segment (PBT). [b] Average segment length of the hard segment calculated according to $l_{HS} = 1/(1 - x_{HS})$.

(PEB) soft block in PBT-based copoly(ether ester)s should result in an extreme phase separation and hence in an increased elasticity. Recently, we reported the successful synthesis of hydrogenated polybutadiene (PEB)-containing PBT-based copolyesters.[20] Macrophase separation during melt condensation was avoided by using a poly(ethylene oxide)-*block*-poly(ethylene-*stat*-butylene)-*block*-poly(ethylene oxide) (PEO-*b*-PEB-*b*-PEO) triblock copolymer. The PEO acts as a compatibilizer between the polar PBT and nonpolar PEB blocks. Here we present a detailed study dealing with the characterization of the PEO-*b*-PEB-*b*-PEO containing PBT-based copolyesters. The formation of a dispersed PBT hard phase by crystallization from a microphase-separated melt will be demonstrated using rheological techniques in combination with small-angle X-ray scattering (SAXS). Morphological studies using transmission electron microscopy (TEM), small-angle X-ray scattering (SAXS), differential scanning calorimetry (DSC), and dynamic mechanical analysis (DMA) as well as scanning force microscopy (SFM) for surface structure analysis will be described. The increase in elasticity will be demonstrated by mechanical characterization.

Experimental Section

Synthesis. Detailed information about the synthesis of PEO-*b*-PEB-*b*-PEO containing copolyesters can be found in a previous contribution.[20] Solid-state postcondensation of copolyesters was performed in vacuum (1−2 mbar) under a slight stream of nitrogen in a home-built apparatus. The copolyesters were cut into small pieces in order to enlarge the active surface, and the reaction was carried out for 2 days at temperatures ca. 30 °C below the melting temperature of the copolyester. The structure of the synthesized copolyesters with PEO-*b*-PEB-*b*-PEO triblock copolymer soft segments is depicted in Figure 1. In this contribution we will focus on copolyesters based on $PEO_{18}PEB_{64}PEO_{18}^{5.6}$ and $PEO_{22}PEB_{56}PEO_{22}^{6.4}$ soft segments. (The subscripts give the weight percentage of the corresponding block, and the superscript is the molar mass of the triblock copolymer in kg/mol.) Several copolyesters with varying hard segment content have been synthesized (Table 1). PBT1000/50, a copoly(ether ester) containing 50% (w/w) PTMO with a molecular weight of 1000 g/mol, is used as reference material for comparison of elastic properties. The nomenclature of the new materials like PBT45-1000 is as follows: 45 is the weight percentage of PBT, and 1000 refers to the molecular weight of the PEO block (in g/mol).

Dynamic Mechanical Analysis (DMA). For the determination of glass transition temperatures, a Rheometrics DMTA IV operated in the rectangular torsion/compression mode at a heating rate of 2 K/min, and a constant frequency of 10 rad/s was used. Sample films with dimensions of 6 × 15 × 0.5 mm were used. Given glass transition temperatures correspond to a maximum in the loss modulus (E''), unless otherwise specified. Dynamic shear experiments were performed with an Advanced Rheometric Expansion System (ARES, Rheometrics) in the plate−plate configuration. For measurements on copolyesters a plate diameter of 25 mm and a gap of 1.5 mm were used. Temperature-dependent measurements of G' and G'' were performed at a scanning rate of 1 K/min at a constant frequency of 1 rad/s. PEO-*b*-PEB-*b*-PEO triblock copolymers were measured using 50 mm plates with a gap of 1 mm at a scanning rate of 1 K/min at a constant frequency of 0.5 rad. Order−disorder transitions were detected by a sharp drop of G' and G'' upon heating. Given order−disorder transition temperatures correspond to the crossover of G' and G'', i.e. $G' = G''$. It was made sure that all experiments were done in the linear viscoelastic regime.

Differential Scanning Calorimetry (DSC). For thermal analysis a Perkin-Elmer DSC 7 with a CCA 7 liquid nitrogen cooling device was used. For all measurements a two-point calibration with chloroform and indium was applied. All experiments were performed at heating rates of 20, 30, and 40 K/min. Given transition temperatures correspond to an extrapolated heating rate of 0 K/min, unless otherwise specified. Degrees of crystallinity were calculated assuming a heat of fusion of $\Delta H_m^0 = 196.6$ J/g[21] for PEO and $\Delta H_m^0 = 145.3$ J/g[22] for PBT.

Transmission Electron Microscopy (TEM). The bulk morphology of copolyesters was examined by bright field TEM using a Zeiss CEM 902 electron microscope operated at 80 kV in the bright field mode. Films (around 1 mm thick) were prepared by compression molding at 240 °C for 5 min followed by cooling to room temperature (ca. −20 K/min) in an identical manner compared to the preparation of test specimens for tensile testing. Thin sections were cut at −130 °C using a Reichert-Jung Ultracut E microtome equipped with a diamond knife. Staining was achieved by exposure of the sections to RuO_4 vapor for 45 min. Since the staining agent penetrates only into the amorphous regions, the crystalline PBT domains appear bright.

Scanning Force Microscopy (SFM). Scanning force microscopy images were taken on a Digital Instruments Dimension 3100 microscope operated in Tapping Mode (free amplitude of the cantilever, 20 nm; set point ratio, 0.95). Measurements were performed on compression-molded films prepared on polished silicon wafers using poly(tetrafluoroethylene) (PTFE) cover sheets. The samples were first heated to 250 °C for 3 min under nitrogen followed by cooling at a constant rate of 5 K/min to room temperature.

Small-Angle X-ray Scattering (SAXS). SAXS was performed on a Bruker-AXS Nanostar equipped with a Histar detector and crossed Goebel mirrors. As a radiation source, a sealed Cu tube was used, generating a wavelength of 0.1542 nm. Temperature-dependent measurements were conducted using a Paar Physica TCU50 temperature control unit.

Mechanical Testing. Mechanical testing was carried out on a Zwick 1455 tensile testing machine equipped with optical extensometers and a 200 N load cell. Hysteresis measurements were performed at a testing speed of 100 mm/min with a preload of 1 N without applying a holding time between the cycles in order to reduce relaxation phenomena. Cyclic measurements were performed for 100 and 500% strain and were repeated three times. The geometry of test specimens was based on ISO 37:1994. Samples were pressed into plates by compression-molding between PTFE sheets at 240 °C for 5 min followed by cooling to room temperature (ca. −20 K/min). All samples were allowed to acclimatize at room temperature (23 °C) under a relative air humidity of 50% for 1 day.

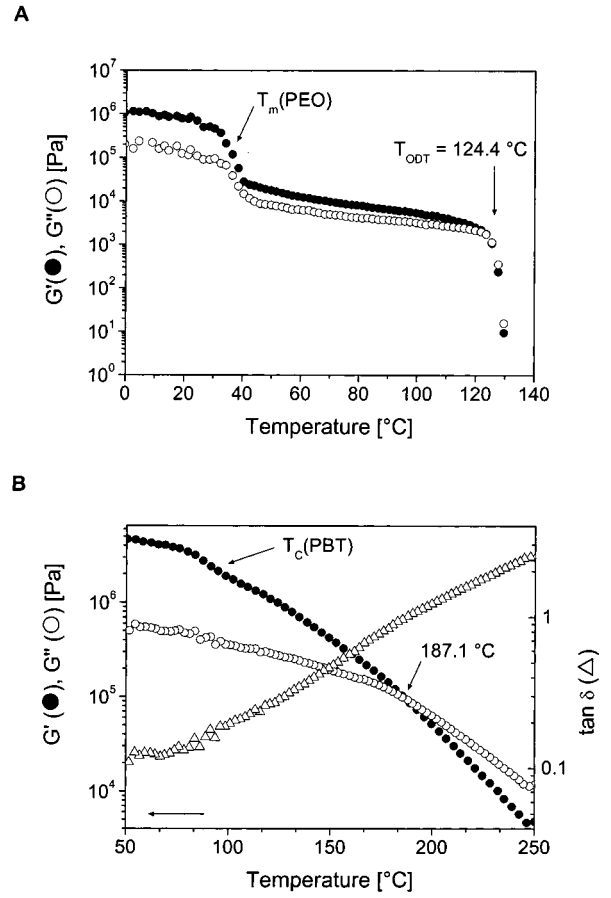

Figure 2. (A) Temperature dependence of storage (G') and loss (G'') modulus for $PEO_{18}PEB_{64}PEO_{18}$[5,6] upon heating. (B) Temperature dependence of storage (G') and loss (G'') modulus for PBT20-1000 upon cooling.

Results and Discussion

Dynamic Shear Experiments. To investigate the structure formation in PEB containing copolyesters upon cooling from the melt, dynamic shear experiments have been performed. The pure PEO-*b*-PEB-*b*-PEO triblock copolymers were measured first as a reference. Figure 2A shows the temperature dependence of storage (G') and loss (G'') modulus for the triblock copolymer $PEO_{18}PEB_{64}PEO_{18}$[5,6]. Upon heating, the crystalline PEO blocks melt at ca. 35 °C, resulting in a simultaneous drop in G' and G''. In the following plateau the modulus is nearly constant up to ca. 124 °C. At this temperature a sharp drop over several decades in both G' and G'' indicates the order−disorder transition (T_{ODT}), resulting in a homogeneous melt.[23−28] The triblock copolymer $PEO_{22}PEB_{56}PEO_{22}$[6.4] exhibits a similar temperature dependence of G' and G'' (results not shown). Because of the increased molecular weight of the PEO blocks, the order−disorder transition shifts to 180 °C. Please note that crystallization of the PBT hard segments in the PEB containing copolyesters occurs below the observed order−disorder transition for the soft segments (Table 2). This might indicate that crystallization of PBT occurs from a microphase-separated melt consisting of pure PEB domains and mixed PBT/PEO domains. (Amorphous PBT and PEO domains are miscible in the melt.)

Figure 2B shows the dependence of G' and G'' on temperature for PBT20-1000 upon cooling. In this case no sharp rise in G' upon cooling, which would indicate an order−disorder transition, can be detected. For high temperatures the viscous response of the melt predominates, i.e., $G'' > G'$. Upon cooling at ca. 187 °C a crossover point can be detected, i.e., $G' = G''$. Below this temperature the elastic response of the melt prevails, i.e., $G' > G''$, indicating that either entanglements become active or the melt microphase separates, leading to a thermoreversible network. Upon further cooling the PBT hard segments start to crystallize, resulting in a rise in G' at ca. 90 °C, which points to a crystallization of PBT from a microphase-separated melt. The copolyesters PBT45-1000 and PBT20-1380 show a similar temperature dependence of G' and G'' upon cooling (results not shown). The crossover of G' and G'' is shifted to higher temperatures compared to PBT20-1000, i.e., 205 °C for PBT45-1000 and 215 °C for PBT20-1380. This might be attributed on one hand to the increased average hard segment block length in PBT40-1000 and on the other hand to the higher molecular weight of the incorporated triblock copolymer soft segment in PBT20-1380 (Table 1), which is equivalent to a higher viscosity and an increased incompatibility between the components. The melt rheology of copoly(ether ester)s consisting of PBT hard segments and PTMO soft segments is significantly different. Veenstra et al.[7] showed that for these materials crystallization occurs from a homogeneous melt. Temperature-dependent dynamic shear experiments revealed that upon cooling from the homogeneous melt a sharp rise in G' is observed, resulting from crystallization of the hard segment. Here, microphase separation is induced by crystallization of the hard segment and not by liquid−liquid demixing of incompatible chain segments. A similar behavior is observed for the copoly(ether ester) PBT1000/50 (not shown here). In conclusion, for PEO-*b*-PEB-*b*-PEO containing copolyesters crystallization of the PBT hard segments might occur from a microphase-separated melt due to the fact that crystallization of PBT takes place at temperatures well below the order−disorder transition of the incorporated triblock copolymer soft segment (Table 2).

Small-Angle X-ray Scattering. To gain more insight into the melt structure of the synthesized copolyesters, SAXS investigations on the PEO-*b*-PEB-*b*-PEO triblock copolymers and the corresponding copolyesters have been performed. Measurements on the triblock copolymers have been conducted at 80 °C taking into account that the PEO blocks are molten at room temperature in the corresponding copolyesters (Table 2). The semilogarithmic SAXS profile for $PEO_{18}PEB_{64}PEO_{18}$[5,6] at 80 °C (molten PEO blocks) exhibits reflex positions at ratios of $1:\sqrt{3}:2:\sqrt{7}$, which are typical for hexagonally packed cylinders (Figure 3A). The SAXS profile of PBT20-1000 at 30 °C (Figure 3A) shows no distinct reflexes pointing to a cylindrical structure arising from the incorporated soft segment. Only a very broad intensity distribution can be detected which may arise from an overlap of reflexes from interlamellar PBT spacings and reflexes originating from the cylindrical domains in the triblock copolymer soft segment. The corresponding measurement at 250 °C (molten PBT blocks) shows a broad reflex at $q = 0.56$ nm^{-1}, indicating a microphase separation in the melt. The reflex position is slightly shifted to higher spacings compared to the q_{100} reflex of the pure triblock copolymer which can be attributed to the chain extension of the PEO block with PBT units in the copolyester. Because of the lack of

Table 2. Transition Temperatures [°C] for Copolyesters Obtained by DSC and DMA[a]

	T_G (DSC)	T_G^1 (DMTA)	T_G^2 (DMTA)[b]	T_G^3 (DMTA)	T_m (PEO)	T_m (PBT)	T_c^1 (PBT)[c]	T_c^2 (PBT)[c]	T_c^3 (PBT)[c]	α(PBT) [%]
PEB	−62	−52								
PEO	−67/−27[22]	–								
PBT	45[29]	–								
PBT1000/50[d]	−64	−62	–	–	–	190	123	–	–	50
PBT45-1000	−57.6	−51.4	n.d.	47.5	6.1	217.5	–	93.3	58.3	27.3
PBT40-1000	−58.2	−50.9	−8.0	53.8	3.4	211.4	–	89.9	52.6	21.8
PBT35-1000	−58.0	−53.6	−11.0	52.1	4.2	213.5	–	89.9	54.3	23.3
PBT30-1000	−58.1	−51.3	−7.0	53.4	4.9	212.1	126.3	85.9	58.3	27.8
PBT25-1000	−59.1	−53.4	n.d.	n.d.	10.8	214.9	136.3	83.6	60.6	31.1
PBT20-1000	−59.8	−51.0	−7.0	n.d.	5.5	190.0	–	–	60.6	27.0
PBT40-1380	−66.1	−51.3	−7.0	48.5[e]	7.0	207.7	–	97.9	–	15.8
PBT30-1380	−66.5	−52.7	−10.0	42.2[e]	3.8	202.5	–	97.3	62.6	24.0
PBT20-1380	−60.3	−50.3	n.d.	n.d.	13.5	184.0	–	–	56.3	21.9

[a] T_G = glass transition temperature, T_m = melting point of corresponding block (peak maximum), T_c = crystallization temperature of corresponding block (peak maximum), and α = degree of crystallinity. Order−disorder transition temperatures (T_{ODT}) of soft segments determined by dynamic shear experiments: $PEO_{18}PEB_{64}PEO_{18}^{5.6}$, T_{ODT} = 124.4 °C; $PEO_{22}PEB_{56}PEO_{22}^{6.4}$, T_{ODT} = 180.4 °C. [b] Shoulder of main relaxation T_G^1. [c] Crystallization temperatures correspond to a cooling rate of 20 K/min. [d] DSC experiments were performed at a scanning rate of 10 K/min; DMA measurements correspond to a heating rate of 5 K/min at a constant frequency of 1 rad/s. [e] Very weak, determined from maximum in tan δ.

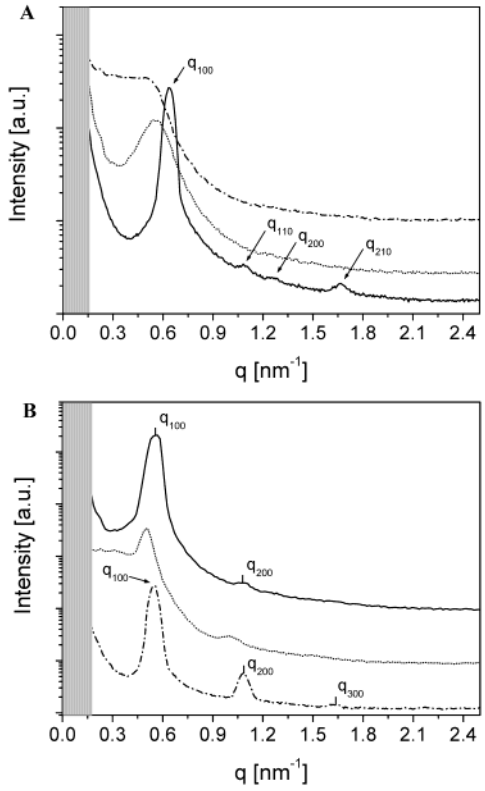

Figure 3. Semilogarithmic SAXS profiles: (A) $PEO_{18}PEB_{64}PEO_{18}^{5.6}$ at 80 °C (—), PBT20-1000 at 30 °C (- · -) and 250 °C (· · ·); (B) $PEO_{22}PEB_{56}PEO_{22}^{6.4}$ at 80 °C (- · -), PBT20-1380 at 30 °C (· · ·) and 250 °C (—); scattering vector $q = 4\pi/\lambda \sin \Theta$ with the scattering angle 2Θ and $\lambda = 0.1542$ nm.

higher order reflexes, a structure assignment is not possible in this case.

The semilogarithmic SAXS profile of $PEO_{22}PEB_{56}PEO_{22}^{6.4}$ at 80 °C exhibits reflex positions at ratios of 1:2:3 typical for a lamellar structure (Figure 3B). The SAXS profile of PBT20-1380 at 30 °C (Figure 3B) shows a broad intensity distribution up to $q \sim 0.4$ nm^{-1}, which might correspond to interlamellar PBT spacings. In addition, two sharp reflexes can be detected at a ratio of 1:2 pointing to a lamellar structure which can also be seen in TEM investigations as will be discussed later. The corresponding lamellar spacing (12.6 nm) is slightly shifted to higher values compared to that of the pure triblock copolymer (11.4 nm). The measurement at 250 °C (molten PBT blocks) reveals a microphase-separated melt with a lamellar structure corresponding to the observed reflex positions at a ratio of 1:2 (Figure 3B). In conclusion, the SAXS experiments confirm the results obtained from dynamic shear experiments, and it can be deduced that crystallization of PBT occurs from a microphase-separated melt.

Transmission Electron Microscopy. To investigate whether crystallization from the observed microphase-separated melt results in the formation of a dispersed PBT hard phase, TEM experiments have been performed. Figure 4 shows TEM images for several copolyesters based on $PEO_{18}PEB_{64}PEO_{18}^{5.6}$ (PBTx-1000) and $PEO_{22}PEB_{56}PEO_{22}^{6.4}$ (PBTx-1380) soft segments. As the staining agent (RuO_4) gets preferentially adsorbed by the amorphous PBT and PEO segments in the soft segment phase, the crystalline PBT and amorphous PEB domains appear as bright regions. As depicted for PBT45-1000 in Figure 4A, the spherical, bright appearing, crystalline PBT domains are dispersed within a matrix of the soft segment. However, because of the selective staining of the amorphous soft segment phase, no fine structure of the crystalline PBT domains can be observed. Comparison with PBT35-1000 (Figure 4B) shows that the number density of crystalline PBT domains decreases as expected with decreasing PBT content. A closer look to the soft segment rich regions in PBT35-1000 indicates a microstructure within the soft segment phase, which is seen as white fine structure in the amorphous phase and originates from the unstained PEB domains. From the TEM image no conclusions can be drawn about the kind of microstructure visible in the soft segment phase. Taking into account that the incorporated triblock copolymer exhibits a cylindrical structure (Figure 3A), the observed microstructure in the soft segment phase might be attributed to a kind of distorted cylindrical structure, which will be underlined in the discussion of the SFM results. Figure 4C,D shows the corresponding TEM micrographs of PBT40-1380 and PBT30-1380. The dispersed crystalline PBT domains are clearly visible. In addition, Figure 4D shows that the soft segment phase exhibits a lamellar microstructure which is in line with SAXS investigations of the incorporated triblock

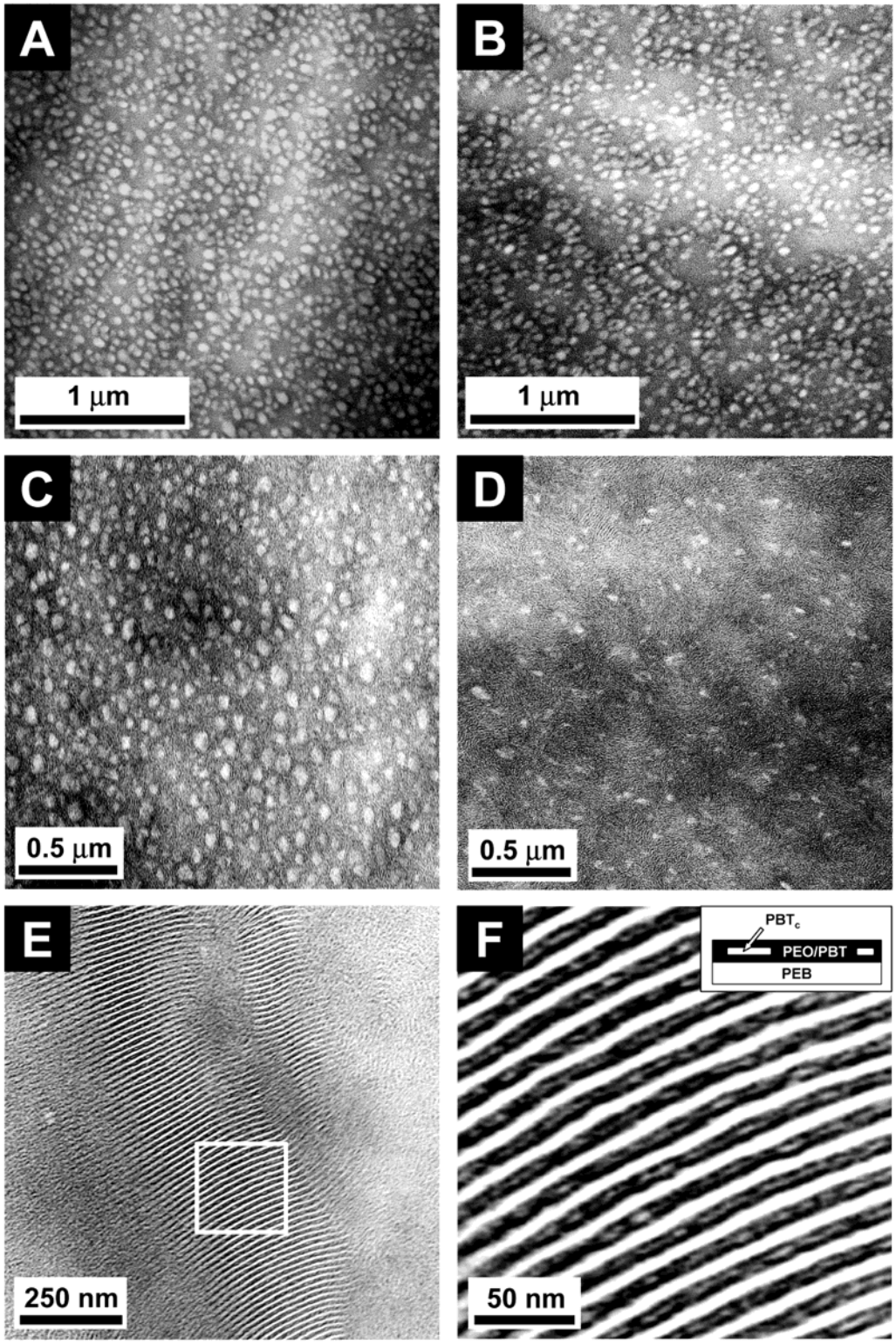

Figure 4. TEM images of PBT45-1000 (A), PBT35-1000 (B), PBT40-1380 (C), PBT30-1380 (D), and PBT20-1380 (E and F, PBT_c = crystalline PBT) stained with RuO_4 vapor.

copolymer (Figure 3B). This lamellar microstructure is more pronounced in PBT20-1380 (Figure 4E,F), emphasizing the strong influence of the incorporated triblock copolymer on the morphology of the copolyester. Figure 4F shows the lamellar microstructure of PBT20-1380 in more detail. The bright lamellae correspond to the nonpolar PEB, which is not stained by RuO_4. The dark appearing lamellae accord with the amorphous PEO/PBT mixed phase and show some white "inclusions" which might be attributed to thin crystalline PBT lamellae (denoted as PBT_c in Figure 4F). This assumption is supported by an increase of the long spacing from 11.4 nm in the pure triblock copolymer to 12.6 nm in PBT20-1380 as derived from SAXS measurements (Figure 3B). In conclusion, TEM investigations show that the PBT hard phase in the PEO-*b*-PEB-*b*-PEO containing copolyesters is dispersed within a matrix of the soft phase.

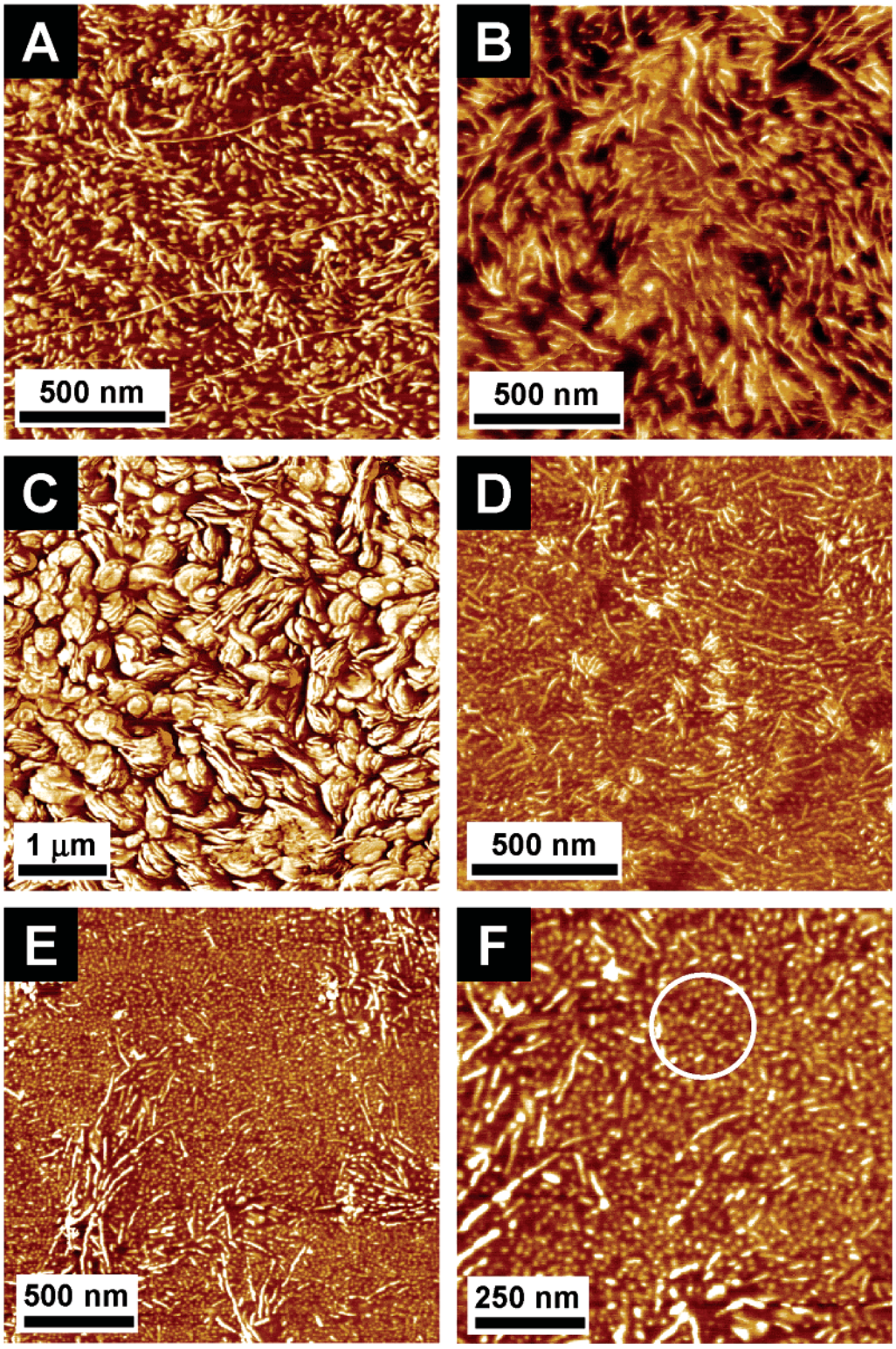

Figure 5. SFM phase contrast images of PBT45-1000 (A: *z* range = 60°), PBT40-1380 (B: *z* range = 50°), PBT45-1000 prepared without a PTFE cover sheet (C: *z* range = 40°), PBT30-1000 (D: *z* range = 30°) and PBT20-1000 (E: *z* range = 20°; F: *z* range = 15°, circle = soft segment phase showing PEO cylinders (bright dots)).

Scanning Force Microscopy. To analyze the fine structure of the crystalline PBT domains, which appears bright using TEM analysis, scanning force microscopy (SFM) has been performed. An additional advantage of using SFM is the elimination of possible cutting effects that could be introduced by the sample preparation for TEM, especially for these soft materials. Figure 5 shows several SFM phase contrast images of copolyesters based on $PEO_{18}PEB_{64}PEO_{18}$[5.6] (PBTx-1000) and PEO_{22}-$PEB_{56}PEO_{22}$[6.4] (PBTx-1380) triblock copolymer soft segments. The phase contrast images of PBT45-1000 (Figure 5A) and PBT40-1380 (Figure 5B) clearly show that the bright appearing elongated domains, which correspond to crystalline PBT lamellae (viewed edge on), are dispersed within a matrix of the soft segment. This is in agreement with the results obtained by TEM

(Figure 4A,C). At this point it has to be mentioned that the SFM experiments were performed on compression-molded films using PTFE cover sheets. As PTFE is a very nonpolar polymer, the also nonpolar PEB blocks have a strong tendency to accumulate at the surface in order to reduce the surface tension. The effect of PTFE on the surface structure is clearly visible in Figure 5C, showing a compression-molded film of PBT45-1000 which was again molten and crystallized without using a PTFE cover sheet. The surface almost completely consists of crystalline PBT lamellae, which agglomerate into more or less globular domains and are dispersed in a matrix of the soft segment. In addition, the lamellar fine structure of the crystalline PBT domains is visible. This structure is very similar to the bright spherical PBT domains observed in TEM investigations (Figure 4A), whereas in the TEM micrographs the lamellar fine structure is not visible. Figure 5D shows the SFM phase contrast image obtained for PBT30-1000. In analogy to PBT45-1000, the crystalline PBT lamellae (bright appearing elongated domains) are again dispersed within a matrix of the soft segment and sometimes form aggregates consisting of several lamellae. This aggregation of several crystalline lamellae might also explain the observed spherical PBT domains in the TEM investigations. As it is not possible to resolve the lamellar fine structure by TEM, the aggregates appear as bright spherical domains. A closer look to the regions rich in soft segment reveals the existence of a microstructure in the soft phase as was also concluded from TEM investigations on PBT35-1000 (Figure 4B). A more detailed insight into the microstructure of the soft segment phase is given in Figure 5E,F showing SFM phase contrast images of PBT20-1000. The bright elongated domains again correspond to crystalline PBT lamellae viewed edge on, which tend to form aggregates consisting of several lamellae. A zoom into the soft segment phase as depicted in Figure 5F clearly shows a microstructure within the soft segment. Inside a dark appearing matrix (lower phase shift) bright spherical domains can be detected which might be attributed to PEO cylinders within a matrix of the PEB block (circle in Figure 5F). This is in line with the SAXS result on the pure $PEO_{18}PEB_{64}PEO_{18}$[5.6] triblock copolymer discussed before (Figure 3A). In summary, dynamic shear and SAXS experiments demonstrate that the morphology in these PEO-*b*-PEB-*b*-PEO containing copolyesters originates from a microphase-separated melt. This in turn results in a dispersed PBT hard phase, as observed by TEM and SFM investigations.

Differential Scanning Calorimetry and Dynamic Mechanical Analysis. To investigate the phase behavior of the different PEB containing copolyesters, DMA and DSC[20] measurements have been performed. Dynamic mechanical analysis of copolyesters with $PEO_{18}PEB_{64}PEO_{18}$[5.6] (PBTx-1000, Figure 6A) and $PEO_{22}PEB_{56}PEO_{22}$[6.4] (PBTx-1380, Figure 6B) soft segments shows for all samples a sharp glass transition temperature at approximately −60 °C. Above this temperature an extended rubber plateau is observed, which is typical for copoly(ether ester)-like elastomeric materials. At temperatures above 150 °C (Figure 6A) melting of crystalline PBT segments starts, resulting in a marked drop in the storage modulus. These observed glass transition temperatures and melting points correspond with the detected transition temperatures using DSC (Table 2). For PBTx-1000 (Figure 6A) and PBTx-1380

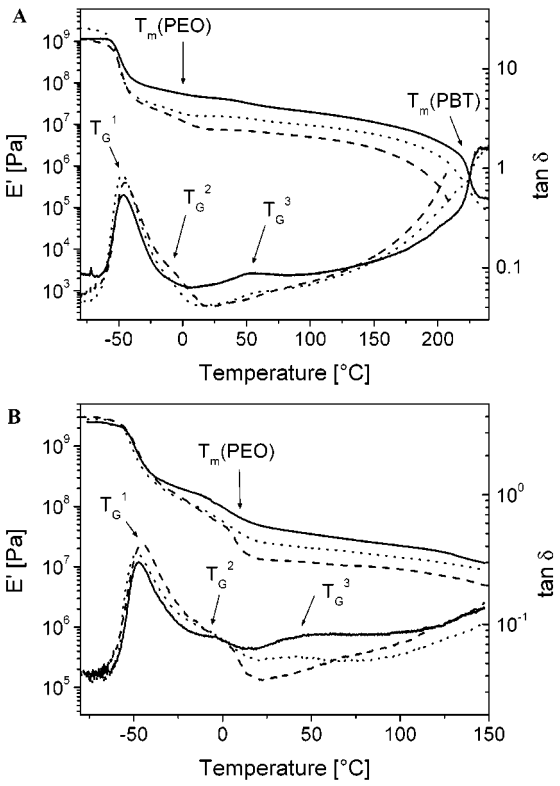

Figure 6. DMA measurements for copolyesters with (A) $PEO_{18}PEB_{64}PEO_{18}$[5.6] soft segments (PBTx-1000): PBT45-1000 (—), PBT35-1000 (• • •), PBT20-1000 (- - -); (B) $PEO_{22}PEB_{56}PEO_{22}$[6.4] soft segments (PBTx-1380): PBT40-1380 (—), PBT30-1380 (• • •), PBT20-1380 (- - -).

(Figure 6B) the storage modulus at room temperature reveals only a slight decrease with decreasing PBT content, reflecting the disperse PBT phase. A closer look to the DMA traces shows that below the melting point of PBT four separate transitions can be distinguished (Figure 6A,B, Table 2). The first glass transition temperature T_G^1 at ca. −60 °C can be attributed to the PEB phase. This glass transition temperature is independent of composition, revealing a strongly phase-separated PEB phase. The loss tangent shows that this first relaxation is not symmetric but shows a shoulder at higher temperatures. This shoulder at ca. −10 °C (T_G^2) might be attributed, in analogy to PTMO containing copoly(ether ester)s,[14] to the glass transition of a mixed amorphous PEO/PBT phase. In the temperature region between 0 and 15 °C the storage modulus E' exhibits a drop. This is more obvious for the polymers PBT20-1000 (Figure 6A) and PBT20-1380 (Figure 6B), possessing higher soft segment contents. Comparison with DSC results (Table 2) shows that this transition can be ascribed to the melting of the PEO blocks. The appearance of a PEO melting point indicates the presence of a PEO-rich phase besides the mixed amorphous PEO/PBT phase, which allows crystallization of PEO as observed by DSC.[20] A third glass transition temperature (T_G^3) can be observed at ca. 50 °C, as indicated by a small drop in E' and a corresponding maximum in tan δ. This glass transition is more pronounced for copolyesters PBTx-1000 with a high PBT content (Figure 6A). In the samples PBTx-1380 (Figure 6B) the transition region is probably very broad. For PBT homopolymer the glass transition temperature is 45 °C.[29] Therefore, the observed third glass transition temperature T_G^3 can be attributed to a pure amorphous PBT phase. A corre-

Table 3. Elastic Properties of Copolyesters Obtained by Cyclic Stress−Strain Measurements[a]

	$\epsilon_{plast}(100)$ [%]	$\epsilon_{plast}(500)$ [%]	$E_{initial}$ [MPa]	E_{100} [MPa]	$E_{100}/E_{initial}$ [%]
PBT1000/50	32.4 (0.2)	314 (1.0)	73.2 (2.5)	20.4 (0.3)	27.9
PBT40-1000	5.9 (0.2)	−	15.2 (1.0)	11.2 (0.4)	73.7
PBT35-1000	4.2 (0.2)	−	12.0 (0.6)	10.2 (0.2)	85.0
PBT30-1000	4.7 (0.2)	−	12.2 (0.2)	9.3 (0.2)	76.2
PBT25-1000	8.3 (0.3)	−	13.9 (1.0)	9.5 (0.5)	68.3
PBT20-1000	2.8 (0.1)	104 (0.5)	8.7 (0.1)	7.5 (0.1)	86.2
PBT25-1000_P[b]	4.6 (0.2)	−	9.3 (0.1)	8.5 (0.1)	91.4
PBT20-1000_P[b]	0.6 (0.1)	−	6.9 (0.2)	6.6 (0.2)	95.7

[a] $\epsilon_{plast}(x)$ = remaining plastic deformation after a cyclic extension to x %; $E_{initial}$ = initial Young modulus; E_{100} = initial Young modulus for the second cyclic extension to 100% strain; values in parentheses give the standard deviations. [b] Samples were subjected to a solid-state postcondensation.

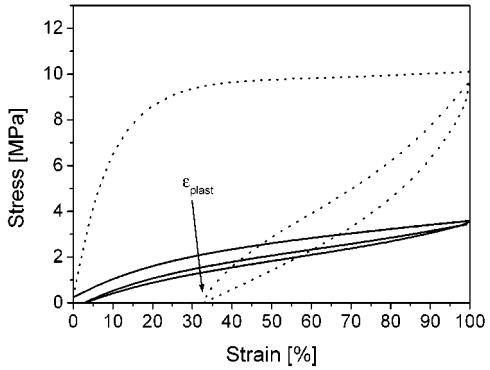

Figure 7. Comparison of hysteresis measurements up to 100% strain for PBT20-1000 (—) and PBT1000/50 (· · ·).

sponding transition in the second DSC heating traces is not detectable (Table 2). However, this transition is visible in the first heating trace or after annealing at temperatures slightly below the glass transition temperature of PBT for copolyesters with PBT contents ≥ 30 wt % (results not shown). The results obtained by DSC and DMA experiments refine the morphology picture obtained by TEM and SFM. The following structure can be proposed. The copolyesters with PEO-*b*-PEB-*b*-PEO soft segments consist of a crystalline PBT phase and an amorphous phase, which can be divided into a pure PEB phase, a PEO-rich phase besides a mixed PEO/PBT phase, and a pure amorphous PBT phase. To provide more evidence for the existence of these proposed different phases, the PEB containing PBT-based copolyesters have been studied in more detail using solid-state NMR. These results will be presented elsewhere.[30]

Mechanical Characterization. TEM and SFM investigations show that in the PEB containing copolyesters the hard phase is dispersed within a matrix of the soft phase. Compared to the co-continuous hard phase in PBT−PTMO-based copoly(ether ester)s like PBT1000/50, a dispersed hard phase should result in a better elastic recovery. To prove this assumption, hysteresis measurements have been performed on copolyesters with $PEO_{18}PEB_{64}PEO_{18}$[5.6] soft segments. Figure 7 shows a comparison of hysteresis measurements up to 100% strain for PBT20-1000 and PBT1000/50. The course of the traces underline the disperse and co-continuous morphology found for PBT20-1000 and PBT1000/50, respectively. At any strain value PBT20-1000 exhibits a smaller stress value compared to PBT1000/50; i.e., PBT20-1000 is a "softer" material. Comparing the obtained plastic deformations (ϵ_{plast}) after elongation to 100%, PBT20-1000 shows a significantly lower plastic deformation. As depicted in Table 3, all copolyesters based on $PEO_{18}PEB_{64}PEO_{18}$[5.6] soft segments reveal a significantly lower plastic deformation compared to that of PBT1000/50. This effect is visible not only at 100% elongation but also, and even more pronounced, at 500% elongation (Table 3). Increasing the molecular weight by solid-state postcondensation results in an additional improvement, as is demonstrated by the postcondensated samples PBT20-1000_P and PBT25-1000_P (Table 3). The significantly increased elasticity results not only from the increased amount of soft block (due to the less extreme phase separation between PBT and PTMO, incorporation of a higher amount of PTMO will result in a homogeneously mixed system) but also mainly from differences in the hard segment structure. The co-continuous hard phase in PBT1000/50 is much easier irreversibly disrupted upon elongation compared to the disperse hard phase in PEO-*b*-PEB-*b*-PEO-based copolyesters, resulting in a much higher plastic deformation.

An irreversible disruption of the hard phase in the PEB containing copolyester should result in a so-called strain softening effect. This effect is reflected by a decrease of the "second" initial modulus in the second cycle of a hysteresis test compared to the original initial modulus.[31,32] Table 3 shows a comparison of the original Young modulus ($E_{initial}$) and the "second" initial modulus in the second cycle after an elongation to 100% (E_{100}). The copolyesters based on $PEO_{18}PEB_{64}PEO_{18}$[5.6] soft segments exhibit a significantly lower decrease in the "second" initial modulus E_{100} compared to that of PBT1000/50. This supports the assumption that a dispersed PBT hard phase undergoes less irreversible disruption upon elongation compared to a co-continuous hard phase.

Conclusions

We have investigated the morphology and elastic properties of several PBT-based copolyesters with PEO-*b*-PEB-*b*-PEO soft segments. Dynamic shear experiments in combination with small-angle X-ray scattering show that crystallization of the PBT hard segments occurs from a microphase-separated melt. This results in a dispersed hard segment phase within a matrix of the soft phase as revealed by TEM and SFM investigations. DMA and DSC measurements show an enhanced microphase separation in the soft segment phase induced by the nonpolar PEB segments. A structure model can be proposed consisting of a crystalline PBT hard phase and an amorphous soft phase, which can be divided into a pure PEB phase, an amorphous PEO-rich phase besides a mixed PEO/PBT phase, and a pure amorphous PBT phase. Mechanical testing shows a significantly improved elastic recovery compared to the case of PBT1000/50, a copoly(ether ester) exhibiting a co-continuous hard and soft phase structure. This

demonstrates that an increased phase separation, which results here in a disperse PBT hard phase, leads to significantly improved elastic properties.

Acknowledgment. The authors thank J. van Elburg (DSM) for assistance with mechanical testing, A. Böker and Prof. G. Krausch (Physikalische Chemie II) for support concerning the SFM measurements, A. Göpfert (Makromolekulare Chemie II) for TEM investigations, K. Matussek (Makromolekulare Chemie II) and M. Soliman (DSM) for help with rheological analysis, and A. Schmidt (DSM) for helpful discussions. The work was financially supported by DSM Research and in part by the Bayreuther Institut für Makromolekülforschung (BIMF) and the Deutsche Forschungsgemeinschaft (DFG) through SFB 481.

References and Notes

(1) Adams, R. K.; Hoeschele, G. K.; Witsiepe, W. K. In *Thermoplastic Elastomers*; Holden, G., Legge, N. R., Quirk, R., Schroeder, H. E., Eds.; Hanser: Munich, 1996; p 191.
(2) Cella, R. J. *J. Polym. Sci., Polym. Symp.* **1973**, *42*, 727.
(3) Hoeschele, G. K.; Witsiepe, W. K. *Angew. Makromol. Chem.* **1973**, *29/30*, 267.
(4) Hoeschele, G. K. *Chimia* **1974**, *28*, 544.
(5) Seymour, R. W.; Overton, J. R.; Corley, L. S. *Macromolecules* **1975**, *8*, 331.
(6) Zhu, L.-L.; Wegner, G. *Macromol. Chem.* **1981**, *182*, 3625.
(7) Veenstra, H.; Hoogvliet, R. M.; Norder, B.; Boer, A. P. *J. Polym. Sci., Polym. Phys.* **1998**, *36*, 1795.
(8) Soliman, M.; Dijkstra, K.; Borggreve, R. J. M.; Wedler, W.; Winter, H. H. In *Makromolekulares Kolloquium Book of Abstracts*, Freiburg, 1998.
(9) Buck, W. H.; Cella, R. J.; Gladding, E. K.; Wolfe, J. R. *J. Polym. Sci., Polym. Symp.* **1974**, *48*, 77.
(10) Bandara, U.; Droscher, M. *Colloid Polym. Sci.* **1983**, *261*, 26.
(11) Briber, R. M.; Thomas, E. L. *Polymer* **1985**, *26*, 8.
(12) Lilaonitkul, A.; Cooper, S. L. *Rubber Chem. Technol.* **1977**, *50*, 1.
(13) Zhu, L.-L.; Wegner, G. *Makromol. Chem.* **1981**, *182*, 3639.
(14) Gabriëlse, W.; Soliman, M.; Dijkstra, K. *Macromolecules* **2001**, *34*, 1685.
(15) Pesetskii, S. S.; Jurkowski, B.; Olkhov, Y. A.; Olkhova, O. M.; Storozhuk, I. P.; Mozheiko, U. M. *Eur. Polym. J.* **2001**, *37*, 2187.
(16) Wolfe, R. J. *Rubber Chem. Technol.* **1977**, *50*, 688.
(17) Bonart, R. *J. Macromol. Sci., Phys.* **1968**, *B2*, 115.
(18) Dieterich, D. *Polyurethane*; Hanser: Munich, 1983.
(19) Niesten, M. C. E. J.; Bosch, H.; Gaymans, R. J. *J. Appl. Polym. Sci.* **2001**, *81*, 1605.
(20) Schmalz, H.; Abetz, V.; Lange, R.; Soliman, M. *Macromolecules* **2001**, *34*, 795.
(21) Wunderlich, B. *Macromolecular Physics*; Academic Press: New York, 1980; Vol. 3.
(22) Van Krevelen, D. W. *Properties of Polymers*, 2nd ed.; Elsevier: Oxford, 1976.
(23) Rosedale, J. H.; Bates, F. S. *Macromolecules* **1990**, *23*, 2329.
(24) Gehlsen, M. D.; Almdal, K.; Bates, F. S. *Macromolecules* **1992**, *25*, 939.
(25) Riise, B. L.; Fredrickson, G. H.; Larson, R. G.; Pearson, D. S. *Macromolecules* **1995**, *28*, 7653.
(26) Floudas, G.; Hadjichristidis, N.; Iatrou, H.; Pakula, T.; Fischer, E. W. *Macromolecules* **1994**, *27*, 7735.
(27) Adams, J. L.; Graessley, W. W.; Register, R. A. *Macromolecules* **1994**, *27*, 6026.
(28) Adams, J. L.; Quiram, D. J.; Graessley, W. W.; Register, R. A.; Marchand, G. R. *Macromolecules* **1996**, *29*, 2929.
(29) Turi, E. A. *Thermal Characterization of Polymeric Materials*; Academic Press: Orlando, 1981.
(30) Gabriëlse, W.; Viola, v. G.; Schmalz, H.; Abetz, V.; Lange, R. *Macromolecules*, in press.
(31) Grady, B. P.; Cooper, S. L. In *Science and Technology of Rubber*; Mark, J. E., Erman, B., Eirich, F. R., Eds.; Academic Press: San Diego, 1978; Chapter 13.
(32) Niesten, M. C. E. J.; Gaymans, R. J. *J. Appl. Polym. Sci.* **2001**, *81*, 1372.

MA011995O